Longitudinal electron bunch profile diagnostics at 45 MeV using coherent Smith-Purcell radiation

G. Doucas,[*] V. Blackmore, B. Ottewell, and C. Perry

Department of Physics, Denys Wilkinson Building, University of Oxford, United Kingdom

P. G. Huggard

Space Science & Technology Department, Rutherford Appleton Laboratory, Didcot, Oxford, United Kingdom

E. Castro-Camus, M. B. Johnston, and J. Lloyd Hughes

Department of Physics, Clarendon Laboratory, University of Oxford, United Kingdom

M. F. Kimmitt

Physics Centre, University of Essex, Colchester, United Kingdom

B. Redlich and A. van der Meer

FOM Institute for Plasma Physics, Nieuvegein, The Netherlands

We have used coherent Smith-Purcell radiation in order to investigate the longitudinal (temporal) profile of the electron bunch at the FELIX facility. Detection of the far-infrared radiation was achieved by a simple and compact experimental arrangement, consisting of an array of 11 room-temperature pyroelectric detectors. Accurate determination of the background radiation, use of high quality optical filters, and an efficient light collection system are essential for this type of experiment. The radiated power is in good agreement with the predictions of the surface current description of this process. It is concluded that 90% of the bunch particles are contained within 5.5 ps, with a temporal profile that could be approximately triangular in shape.

I. INTRODUCTION

The term Smith-Purcell (SP) radiation is used to describe the radiation produced through the interaction of a (usually relativistic) beam of charged particles with a periodic metallic structure, e.g., a grating [1]. It belongs to a broader category of radiative processes, such as transition and diffraction radiation. The existence of the periodic structure causes angular dispersion of the emitted wavelength (λ) according to the observation angle (θ), relative to the particle beam direction. For an observer at *infinity* and for observation in the plane perpendicular to that of the grating (see Fig. 1 for axes and angle convention), the relationship is given by

$$\lambda = \frac{l}{m}\left(\frac{1}{\beta} - \cos\theta\right). \quad (1)$$

The symbol l is the period of the grating, m is the order of the emitted radiation, and $\beta = v/c$ is the relativistic factor. The wavelength region of the emitted radiation depends on the chosen periodicity of the grating and can, therefore, be selected. For fine macroscopic gratings it is in the far-infrared part of the spectrum. These properties, together with the fact that the emission of SP radiation causes minimal disruption to the beam, make SP particularly promising as a diagnostic tool for the determination of

the longitudinal (time) profile of charged particle bunches. SP radiation has already been used to determine the longitudinal profile of 14 ps long bunches at low energies [2,3] and at 15 MeV [4]. The motivation behind the present work is threefold: (a) to extend the previous work to beams of higher energy and shorter bunch length; this is an essential step before progressing to GeV beams, (b) to verify the suitability of room-temperature detectors for the measurement of SP radiation and the consequent simplification of the experimental setup, (c) to explore the validity of the "surface current" treatment of the radiative process in the 45−50 MeV regime.

Knowledge of the time profile of the bunch is particularly important in the context of a future International Linear Collider (ILC) because of "beam-beam" effects. These occur when the colliding bunches of electrons/positrons experience strong electromagnetic fields from the opposing bunch, leading to deflection, beamstrahlung, and emittance growth. Additionally, at the interaction point of the accelerator the beams will experience a "pinch effect" that can focus each beam, resulting in either a reduction or expansion of their size. These effects depend, among other things, on the time profile of the bunch and can have significant consequences on the ILC's luminosity [5].

For the sake of completeness, we summarize briefly the basic ideas underlying the determination of the time profile of a bunch of charged particles through the measurement of
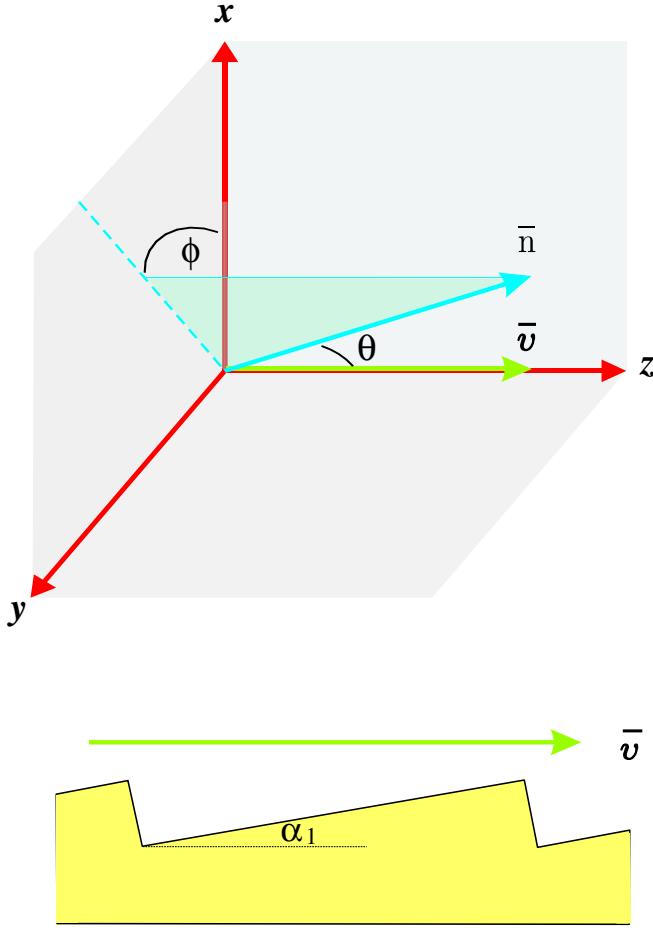
---

[*]Corresponding author.

FIG. 1. (Color) Definition of the coordinate system. The beam propagates along the z-axis and the x-axis is perpendicular to the grating.

the wavelength distribution of coherent SP radiation. There are a number of different theoretical treatments of the SP emission process [6–9]. We concentrate on the one that describes the emission in terms of currents induced on the grating surface by an electron bunch passing close to the surface and perpendicular to the grooves [10–12]. This is a treatment that has provided good agreement between theory and measured radiated power, with the exception of one experiment at about 850 MeV [13] where special circumstances could have affected the results. The starting point is the calculation of the energy dI emitted in solid angle $d\Omega$, arising from the interaction of a *single* electron with a grating of period l and total length Z:

$$\left(\frac{dI}{d\Omega}\right)_1 = 2\pi q^2 \frac{Zl}{n} \frac{1}{\lambda^3} R^2 \exp\left[-\frac{2x_0}{\lambda_e}\right]. \quad (2a)$$

Alternatively, using (1),

$$\left(\frac{dI}{d\Omega}\right)_1 = 2\pi q^2 \frac{Z}{l^2} \frac{n^2\beta^3}{(1-\beta\cos\theta)^3} R^2 \exp\left[-\frac{2x_0}{\lambda_e}\right]. \quad (2b)$$

The symbol R^2 in Eqs. (2a) and (2b) is usually referred to as the "grating efficiency" or "radiation factor" and it represents the field contribution from each tooth. It is thus a complicated function of the grating profile, the emission order, and the emission angle [12]; it is calculated numerically, for each grating, by the analysis code used in the present work. Other quantities appearing in (2a) and (2b) are the charge q, the height of the electron trajectory above the grating surface x_0, the relativistic factor $\gamma = (1 - \beta^2)^{-1/2}$, and the "evanescent wavelength" λ_e defined by

$$\lambda_e = \frac{\lambda}{2\pi} \frac{\beta\gamma}{\sqrt{1 + \beta^2\gamma^2\sin^2\theta\sin^2\phi}}.$$

In order to estimate the energy radiated in the case of a *bunch of N_e electrons*, it is necessary to know the electron distribution in the three dimensions. We define the x-axis as perpendicular to the grating surface and the y-axis is across the surface, parallel to the grating grooves (see Fig. 1). The energy is then given by

$$\left(\frac{dI}{d\Omega}\right)_{N_e} = \left(\frac{dI}{d\Omega}\right)_1 (N_e S_{\text{inc}} + N_e^2 S_{\text{coh}}). \quad (3a)$$

Assuming uncorrelated electron distributions, $\rho(x, y, t = z/v) = X(x)Y(y)T(t)$, the two new quantities in the above expression (3a) are given by

$$S_{\text{coh}} = \left|\int_0^\infty X e^{-(x-x_0)/\lambda_e} dx\right|^2 \left|\int_{-\infty}^\infty Y e^{-ik_y y} dy\right|^2$$
$$\times \left|\int_{-\infty}^\infty T e^{-i\omega t} dt\right|^2 \quad (3b)$$

for "coherent integral" S_{coh}, while the "incoherent integral" S_{inc} is given by

$$S_{\text{inc}} = \int_0^\infty X e^{-2(x-x_0)/\lambda_e} dx,$$

The y-component (k_y) of the wave vector (k) in the coherent integral is given by $k_y = k\sin\theta\sin\phi$ and ω is the angular frequency of the radiation; the quantity x_0 is now defined as the height of the beam center above the grating.

If the bunch length is long compared to the wavelength, the coherent integral S_{coh} is negligible and the shape of the bunch becomes irrelevant. The situation resembles that of a continuous, dilute beam; the contributions of N_e electrons will add together in an incoherent way and the radiated energy will be just $N_e S_{\text{inc}}$ times that of a single electron. For bunched beams whose bunch length is short enough to be comparable to or shorter than the wavelength of the radiation, S_{coh} becomes significant, the second term inside the parenthesis of (3a) dominates and there is "coherent enhancement" of the emitted radiation by a factor approaching N_e:

$$\left(\frac{dI}{d\Omega}\right)_{N_e} \cong \left(\frac{dI}{d\Omega}\right)_1 (N_e^2 S_{\text{coh}}).$$

This will be critically dependent on the last integral in S_{coh}, which is the Fourier transform of the time profile of the bunch. There is, thus, a direct link between the longitudinal profile of the bunch and the wavelength distribution of the radiated power. Measurement of the latter allows the reconstruction of the former. This is the physical basis of this approach to the problem of bunch profile determination. The particularly attractive feature of SP radiation is precisely the fact that, by a suitable choice of period l, the radiation can be made to be coherent. Assuming some prior knowledge of the approximate bunch length, the period of the grating can be matched to it. As a general comment, it should be noted that choosing a period that is much shorter than the bunch length will suppress the coherence effect. On the other hand, choosing a period much longer than the bunch length will result in full coherence of the emitted radiation and consequent loss of the information on the wavelength (angular) distribution of the radiated power. A reasonable first approximation to the optimum period would be one that is roughly equal to or slightly longer than the bunch length. It should be noted that, apart from the fundamental ($m = 1$), radiation is also emitted in higher orders. Therefore, each observation angle receives wavelengths that are harmonics of the fundamental. Compared to the fundamental, the energy radiated in these orders is expected to become progressively lower because of the exponential term in (2a) and because of the reduction in the value of the coherent integral for shorter wavelengths. However, it is possible that this energy may be significant and could be used to extend the wavelength range of the experiment.

In Sec. II of the paper we describe in some detail the experimental setup used in these experiments. The various calibration checks and the analysis of the data are described in Sec. III and, finally, the summary and conclusions are presented in Sec. IV.

II. EXPERIMENTAL

A. Beam parameters

The experiments were carried out at the FELIX facility, FOM Institute, The Netherlands. The Linac delivers beams with energies up to 50 MeV and is usually run in one of two modes. In the ''low frequency'' mode (25 MHz), the bunch spacing is 40 ns, the number of electrons in the bunch is 1.5×10^9, and the maximum energy is 50 MeV. In the ''high frequency'' mode (1 GHz), the bunch spacing is 1 ns, with 1×10^9 electrons per bunch, and with a maximum energy of 45 MeV. Although experiments were carried out at both machine frequencies, the data presented here refer to the high frequency mode (1 GHz) because of the stronger detector signals. The approximate bunch length was expected to be in the range of 1–3 ps. The

bunch train duration, in either mode, was about 5 μs. The beam has a normalized emittance of 100π mm mrad and was brought to a waist at approximately the center of the grating. The size of the waist (FWHM) was determined to be 2 mm in the x-direction and about twice that in the y-direction. The position of the beam center above the grating was 2.5 mm. Focusing of the beam was achieved by adjustment of the upstream quadrupole lenses and observation of the beam shape on a retractable scintillating screen, located about 20 cm downstream from the grating. The beam current was measured at the beam dump, located about 2 m after the grating chamber.

B. Experimental setup

As mentioned previously, the reconstruction of the bunch shape requires the determination of the radiated power over as wide a range of wavelengths as possible. An array of 11 detectors (Sec. II D), was deployed over the angular range 40°–140°, relative to the electron beam direction [see Fig. 2(a)]. The detectors were mounted outside the vacuum chamber on a support structure that also allowed tilting of the whole detector assembly by 10° away from the plane defined by the z-axis and the normal to the grating (x-z plane). Therefore, measurements could be taken at azimuthal angles $\phi = 0$ and $\phi = 10°$. The orientation of the chamber was such that the x-z plane coincided with the horizontal. The detectors were mounted to view in a direction perpendicular to the x-z plane, with SP radiation directed onto the detector by means of a 90° ''elbow'' equipped with a flat mirror at 45° [Fig. 2(b)]. The reason for this orthogonal detector mounting was to allow the use of lead blocks between the chamber and the electronics in order to provide some shielding against x rays. The chamber was 310 mm long and had an internal diameter of 100 mm. A z-cut crystalline quartz window, with dimensions of 210 mm × 50 mm × 6 mm, allowed the radiation to emerge from the vacuum. The experiment was set up immediately after the ''straight-through'' port of the first bending magnet of the accelerator. Therefore, the beam profile was determined in a location before any chicanes and before the undulator.

Three different gratings with periodicities of 0.5, 1.0, and 1.5 mm were used. Each period consisted of two facets, the first with a blaze angle α_1 (see Fig. 1) and with the second facet perpendicular to the first. The blaze angles were 40°, 35°, and 30°, respectively. The gratings were mounted on a ''carousel'' system, inside the chamber (see Fig. 3). In addition to the gratings, the carousel carried a ''blank.'' This was a piece of smooth metal, of identical dimensions to the gratings but without any periodic structure. The gratings and the blank were 40 mm long and 20 mm wide and were machined out of aluminum. A remotely controlled motor allowed retraction of the carousel to its furthest point from the beam axis (50 mm), at which point a ''ratchet and pawl'' mechanism rotated the

(a)

FIG. 3. (Color) The carousel mechanism carrying three gratings and the blank.
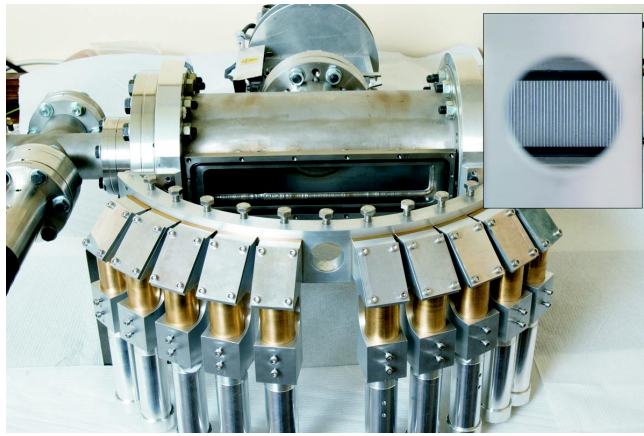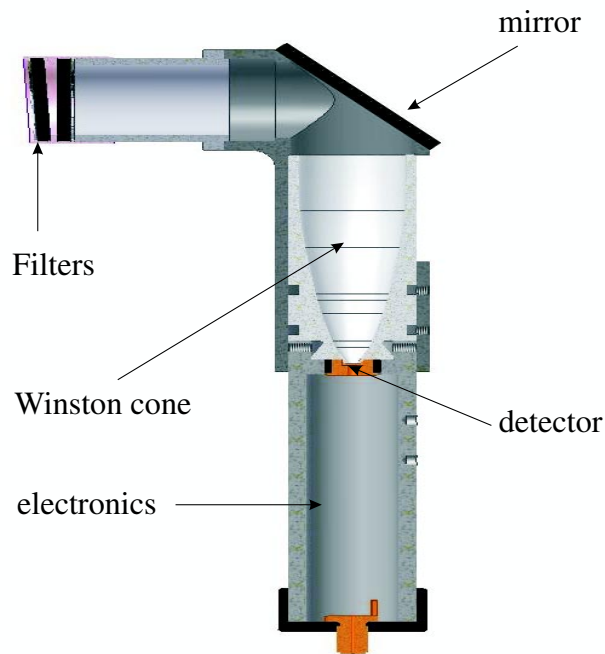
(b)

FIG. 2. (Color) (a) Vacuum chamber and detector array. The inset shows a view of one grating as seen through the 90° port, from which the detector, Winston cone, and bending mirror assembly have been removed. (b) Schematic of 90° elbow and Winston cone.

carousel by 90°. It was thus possible to change over between gratings and blank without breaking the vacuum. This mechanical device proved a very useful tool in establishing the level of the background signal.

C. Background radiation

It became obvious from the early stages of the experiment that "background" radiation was a significant con-
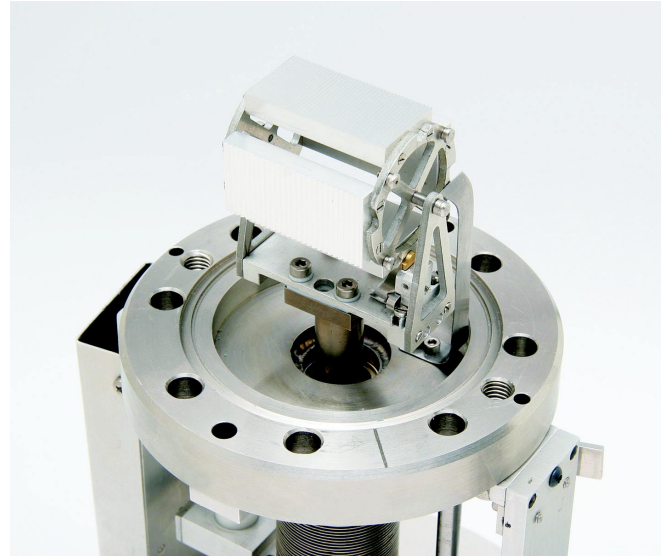
tributor to the power reaching the detectors. Background in the context of this paper means all radiation, whatever its origin that does not arise from the periodic structure itself, i.e., all non-SP radiation. Compared to the SP signal it can be both short and long wavelength. On the short wavelength side, partial suppression of the x-ray contribution was achieved by the use of the previously mentioned 90° elbow and additional lead shielding. Suppression of other short ($\lambda < 100~\mu$m) wavelengths was provided by: (a) the crystalline quartz window itself that only transmits in the far-infrared (FIR) region for $\lambda \geq 70~\mu$m and (b) by a 2 mm thick sheet of Fluorogold, placed over the quartz window, which is transparent in the FIR but cuts off all visible and short infrared wavelengths.

In addition to this, there is background radiation of wavelengths that are comparable with or longer than that of the SP signal. Since the experiment did not involve the use of any additional spectrometer, apart from the dispersive action of the grating itself, effective rejection of the unwanted (especially the long) wavelengths and efficient collection of the SP radiation were essential for any meaningful measurements. It is probable that this background arises from a combination of higher machine harmonics and diffraction radiation from the edge of the grating and from various apertures upstream from the grating chamber. A thorough investigation of its origin was beyond the scope and the time constrains of this project. Therefore, it was decided to simply quantify it and subtract it from the measured signal. This was achieved through the use of: (a) the carousel system for the rapid change between gratings and blank and whose purpose was to provide a measure of the radiation scattered into the detectors, irrespective of the existence of any periodic structure (b) high quality optical filters and (c) nonimaging light concentra-

tors ("Winston cones"). The latter two are described in Sec. II D.

D. The optical system

Waveguide array plate (WAP) filters [14] can be designed to have high transmission ($> 50\%$) at the resonance wavelength, a very sharp transition to the long wavelength cutoff [15] and some suppression of the shorter wavelengths. Fine wire mesh filters, on the other hand, cannot provide the efficient rejection of background while, at the same time, allowing the desired wavelengths to pass through. This is due to the fact that these filters have a rather slow long wavelength cutoff. In an SP experiment the central wavelength at a given observation port varies with the grating period and the order of emission. Therefore, use of three gratings with different periodicities would require, in principle, three separate sets of filters just for observation of the 1st order wavelengths; additional filters would be required for the observation of higher orders. The work reported here was for 1st order radiation and all wavelengths quoted refer to this order. Only two complete sets of filters were available, those for the 1st order of the 0.5 and the 1.0 mm gratings. Note, however, that according to Eq. (1) a given filter may be usable with more than one grating periodicity; when using the 1 mm grating, for example, the 60° port receives the same wavelength range as the 90° port with the 0.5 mm grating. Hence, our set of filters was suitable for all ports and all three grating periodicities, with the exception of the 110° port of the 1.5 mm grating for which wavelength matching was poor and the 120°–140° ports, for which no filters were available. These last three ports were operated either without any filter or, on occasion, with a thick plug made out of aluminum, which provided full suppression of all infrared radiation into the detectors. The WAP filters were designed at the Rutherford Appleton Laboratory and were manufactured in Oxford. Each filter consists of a brass disk, 21 mm in diameter, with a number of holes drilled in it. The number, diameter, and spacing of the holes and the thickness of the disk determine the central and the cutoff wavelengths. The longer the wavelength the smaller the number of required holes and the greater their diameter and disk thickness. The filter for the 70° port (0.5 mm grating), for example, which was designed for a cutoff wavelength of $\lambda = 398$ μm, had a thickness of 0.575 mm and 4167 holes of 0.23 mm diameter. The transmission characteristics of each filter were measured by either "terahertz time domain spectroscopy" (THz-TDS) [16] or by a Fourier transform spectrometer and a liquid helium cooled InSb detector [17]. Figure 4 shows the transmission curve for the previously mentioned filter. Also shown, for comparison purposes, are the transmission characteristics of wire mesh filters having 110, 200, and 500 lines per inch. The superiority of the WAP filter in
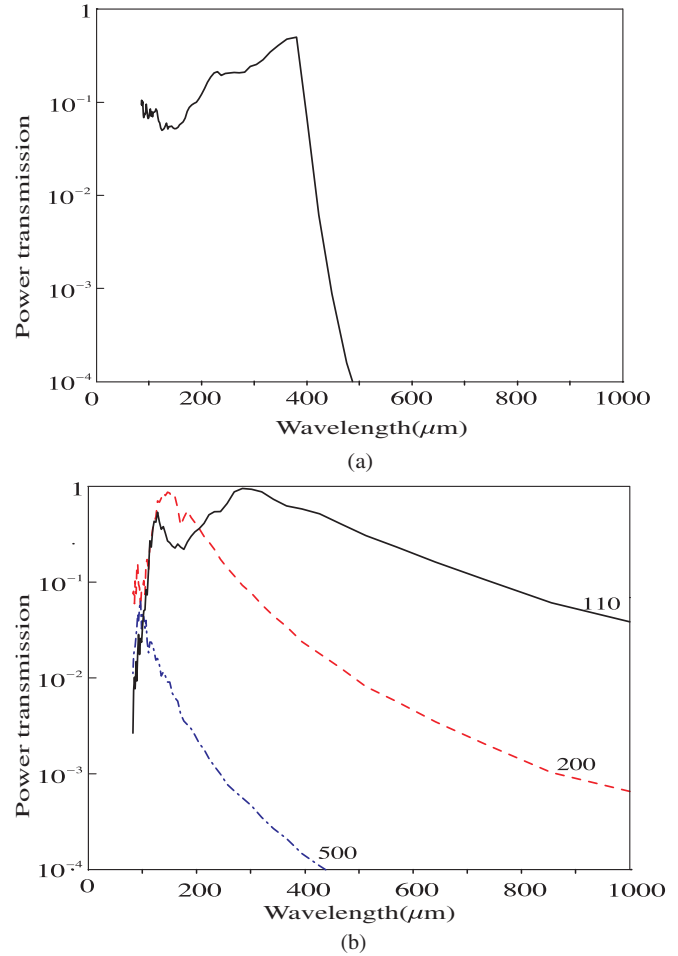

(a)

(b)

FIG. 4. (Color) Terahertz time domain measurements of the power transmission characteristics of: (a) a waveguide array plate filter, designed for a cutoff wavelength of 398 mm and (b) three wire mesh filters with different number of lines per inch.

sharpness of cutoff and enhanced long-wavelength suppression is evident.

Nonimaging light concentrators, in the form of Winston cones, have been described in the literature and have been used in a number of experiments, from Astrophysics to Particle Physics [18–20]. The essential feature of the device is that light entering the entrance aperture within a finite range of incidence angles will (after multiple reflections on the parabolic internal profile of the concentrator) emerge through the exit aperture. The entry and exit angles θ_i and θ_e, respectively, and the entry and exit aperture areas A_i and A_e are related by Liouville's theorem, hence,

$$A_i \sin^2 \theta_i = A_e \sin^2 \theta_e.$$

Assuming 100% reflectivity of the metallic surface, which is valid for the wavelength regime of this experiment, the "concentration factor" can be defined as the ratio of the entrance and exit areas. Since the exit aperture is much smaller than the entrance one, it follows that the range of

exit angles must be larger. Therefore, in order to take advantage of the concentrating power of the device, it is necessary to bring the detector as close as possible to the exit aperture so that the emerging beam is detected before it has had a chance to diverge too much. The parameters of the cones used in the present work were determined by the diameter of the detector element (see following section) and by the maximum angle of incidence on the detector: 2 mm and 60°, respectively. Hence, θ_e was set equal to 60° and the exit diameter equal to 2.8 mm. For mechanical reasons the entrance diameter of the cone was 21 mm; these values define a maximum accepted incident angle of $\theta_i = 6.3°$. With this incident angle and with the grating-cone separation of 230 mm, the effective grating length (at an observation angle of 90°) was restricted to about 30 mm, increasing to 39 mm at the two extreme angles of 40° and 140°. The overall length of the cone was 71.5 mm. The maximum theoretical concentration factor is about 56. It is worth noting that the basic SP formula in Sec. I is valid for an observer at infinity. This is not the case in this experiment where, because of the finite (230 mm) distance between grating and cone, a finite wavelength range could have been accepted. Use of the cone limits the range of angles accepted by the optical system and, in effect, moves the grating further from the detector, thus making the collected radiation more monochromatic. The cones were made of brass.

E. Detectors and electronics

Detection of the SP radiation, averaged over the bunch train, was done exclusively by room-temperature devices. The detectors were of the pyroelectric type (Eltec model 400), with lithium tantalate as the sensing element and with no window on the detector housing. Their capacitance is 30 pF and the active diameter is 2 mm. Use of a room-temperature thermal detector gave low sensitivity, but was both low cost and made possible the simple experimental arrangement. Performance was limited by random noise both from the preamplifier and the detector. The latter was thermal noise mostly from the series resistance of the detector electrodes, which varied considerably between units, but measured typically at least 1 kΩ and contributed as much noise as the preamplifier.

The detector electronics used a simple JFET (2SK117) low-noise input; the output, proportional to incident power with a rise time of 500 ns, went onto a 50 Ω coaxial cable which also supplied DC power. X-ray sensitivity of the JFET was an unanticipated problem. This was dealt with by the introduction of the 90° bend (see II B) and the additional lead shielding, which was a major improvement, though not totally effective. Monitoring of x rays was provided by a silicon photodiode (BPW34).

The detector and electronics were mounted by an SMA coaxial bulkhead connector in an aluminum cylinder 85 mm long by 25 mm diameter. The Winston cone was fixed so its tip extended slightly into the opening of the detector housing, to within about 0.5 mm of the detector element. This assembly was compact and easily mounted, with very good electrical screening. A coaxial cable ran from each detector assembly to a common power and load box in the control room. The output signals were recorded on three digital oscilloscopes (TDS3000 series), triggered in synchronism by the accelerator timing system and set to make a single acquisition, averaging data over a number of triggers (usually 64 but occasionally more). Data was written to floppy disks.

III. ANALYSIS AND DISCUSSION

A. Determination of the SP signal

The results presented here are the average of repeated measurements made with the 1.0 mm, 1.5 mm gratings and with the blank. There was only one run with the 0.5 mm grating, at 1 GHz. "Signal" in the context of this paper and unless otherwise stated, is defined as *the difference between the signals obtained from a grating and the blank, both with the same set of filters*. Figure 5(a) is typical of the detector output, in this case at $\theta = 90°$, $\phi = 0°$. The sharp rise at the leading edge of the pulse is due to x rays originating from misalignment of the leading bunches in the bunch train. In order to minimize its effect, the signal was taken to be the average value of the output in the time interval between 3 and 4 μs. The two traces in Fig. 5(b) were recorded on the same run but on the 120° port, which did not have a filter but was sealed with the thick aluminum plug. Since no infrared radiation can get through the plug, the signals must be due to x rays arising from the beam halo impinging on the grating/blank. Assuming that grating and blank are in exactly the same position relative to the beam centroid and that the beam is stable, these two traces should be identical. The fact that they are not, implies either a slight misalignment or a small drift in beam position, or both (see Sec. III B). It was also observed that the x-ray contribution was higher in the forward direction ($\theta < 80°$). The minimum turn-around time between runs was of the order of a few minutes. It was thus important to establish the stability of the beam conditions over a time period of 10–60 min. This was done by comparing the radiated power from two, nominally identical, runs separated by 10 min. The detector output variations were about ±5 mV. Similar variations were observed over a period of about 1 h. We conclude that there is an uncertainty of the order of ±5 mV. For all observation angles below 80° the signal was smaller than 5 mV, or even negative, indicating that the SP output was low and smaller than the uncertainty in the measurement.

There is already ample experimental evidence on the validity of the basic SP formula (1) and, therefore, no spectroscopic measurements were made. Nevertheless, it was important to establish that the signals observed pos-
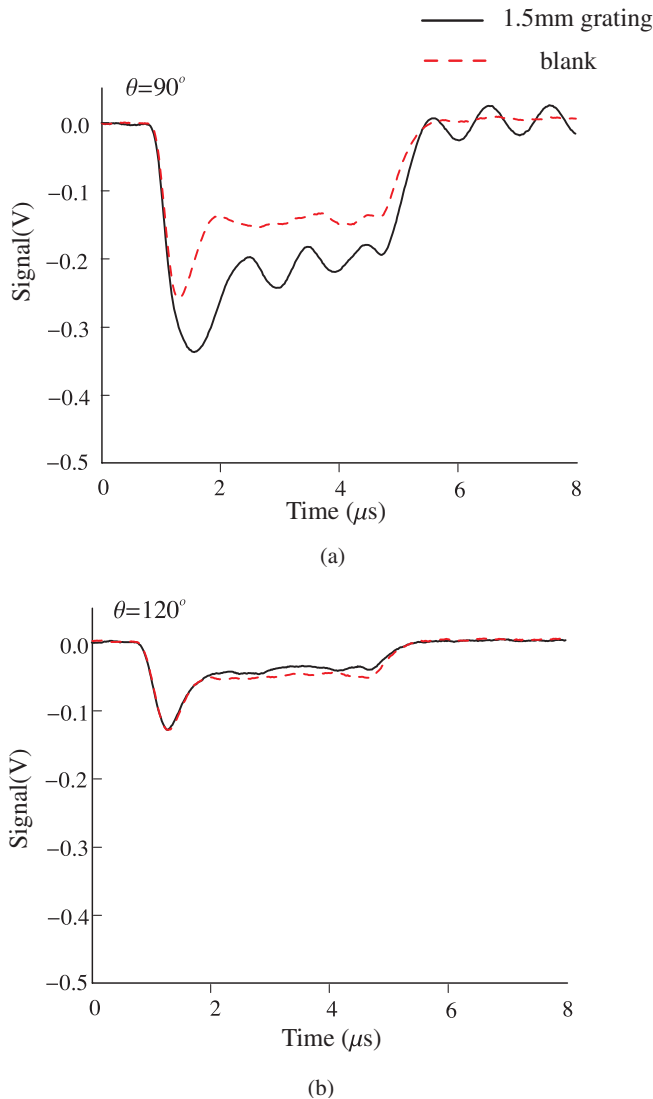
FIG. 5. (Color) (a) Detector output from the 1.5 mm grating and from the blank, using the same set of filters. (b) Detector output from a port sealed with a thick Al plug. The signal is due to x rays (see text for details).

sessed the basic features expected from SP theory. This was confirmed through two different tests. In the first test the signals from the 1 mm grating were recorded on all 11 channels. Some of the filters from the backward angles ($\theta > 90°$) were then swapped with filters from the forward angles, i.e., filters with shorter wavelength cutoff. It was noted that the signal disappeared from the backward angles, thus confirming that the wavelength in these ports was indeed longer than that incident on the forward ports. The second test was based on the fact that SP radiation is sharply peaked in the $\phi = 0°$ plane, especially as the energy of the beam is increased. The detector assembly was rotated to the (nominal) $\phi = -10°$ position and the signals were compared to those of the $\phi = 0°$ plane. The SP signal was completely suppressed by this rotation, in

qualitative agreement with the expectation that it is sharply peaked in the azimuthal plane $\phi = 0°$. The signal from the blank was also reduced to about 25% of its $\phi = 0°$ value, due to the partial obstruction of the Winston cone entry when the detector assembly is rotated. From a simple geometric calculation, this signal should have decreased to about 40% of its original value but this discrepancy can probably be accounted for by the inaccuracy in the determination of the azimuthal angle.

The extraction of the true SP signal is critically dependent on the use of suitable filters. This is evident from Figs. 6(a) and 6(b) which refer to the 1.5 mm grating and the blank. Figure 6(a) shows *separately* the detector output signals from the grating and from the blank. No filters were used for this measurement. The signal from the blank is probably a mixture of diffraction radiation from the edge and scattered radiation. It varies between 0.35 and 0.6 V, approximately; the signals at 40° and 140° are low because of the partial obstruction of these two ports by the edge of the window slot in the vacuum chamber. Insertion of the grating produces an approximately uniform increase in signal of about 40%, in the range $40° \leq \theta \leq 80°$. Thereafter, the increase is significantly higher, reaching about 140% at $\theta = 110°$. However, it would be wrong to ascribe all of the observed increase to SP radiation, because of the absence of filters. Figure 6(b) shows the *net* signal, obtained by subtraction of the signals in 6(a) (full circles). Also shown (squares) is the net signal for an experiment where filters were used in order to isolate the SP component. The conclusion is that for angles $\theta < 80°$ the SP signal is below the level of detection. Hence, the observed increase in Fig. 6(a) in the range $40° \leq \theta \leq 80°$ by the insertion of the grating must be predominantly non-SP radiation. It is known that in transition and diffraction radiation rotation of the edge by θ causes the backward radiation pattern to rotate by 2θ [21]. Therefore, this increase, which is clearly long wavelength, is most probably due to the rotation of the diffraction radiation lobe when the vertical edge of the blank is replaced by the blazed (30°) edge of the grating. When the 1.5 mm grating was used, the 120°–140° ports were left without filters, since no suitable filters were available. We assume that in these three ports the signal is wholly from SP radiation. This can be inferred from Fig. 6(b) which shows, by means of the open crosses, the level of the signal when corrected for filter transmission. The convergence of the filter-corrected SP signal with the unfiltered values for $\lambda > 1.75$ mm is clear. The assumption that the entire signal in the 120°–140° ports is SP radiation, introduces an error (overestimate) of the order of 10%.

The "correction factor" that has to be applied to the measured data in order to account for the filter transmission efficiency is determined from the expected SP wavelength (λ) at a given observation port and from the measured (see Sec. II D) filter characteristics. These values are listed
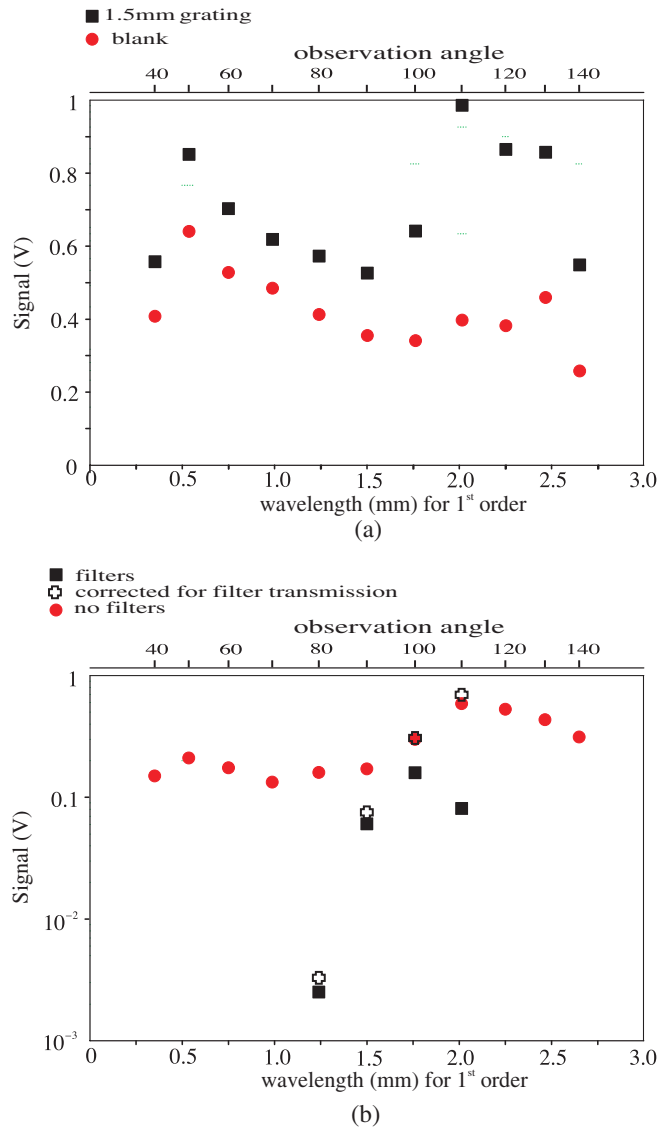
(a)

(b)

FIG. 6. (Color) (a) Signals from the 1.5 mm grating (squares) and from the blank (circles), obtained without the use of filters and (b) the net signal without the use of filters (circles) and with filters (squares). The open crosses represent the signal level when the filter transmission efficiency has been taken into account. See text for details.

below in Table I. The one experimental run with the 0.5 mm grating has low filter transmission efficiencies because the set of filters used was that corresponding to the 1 mm grating. The filters were, therefore, operating on the short wavelength slope of their transmission curve with reduced transmission efficiency.

B. Correction factors

There are three loss mechanisms to be considered in connection with the optical system. The most significant is the loss incurred by the 0.5 mm separation between Winston cone exit and the detector. The Winston cone, or

TABLE I. List of the filter transmission efficiencies applied to the experimental data for various observation angles and different grating periodicities (l). All wavelengths are for order 1.

	$l = 0.5$ mm		$l = 1.0$ mm		$l = 1.5$ mm	
	λ		λ		λ	
θ	(mm)	T	(mm)	T	(mm)	T
40	0.117	0.42	0.234	0.65	0.351	0.57
50	0.179	0.36	0.357	0.59	0.536	0.7
60	0.250	0.38	0.5	0.62	0.75	0.8
70	0.329	0.29	0.658	0.5	0.987	0.8
80	0.413	0.2	0.826	0.79	1.24	0.76
90	0.5	0.2	1	0.8	1.5	0.81
100	0.587	0.23	1.174	0.86	1.760	0.53
110	0.671	0.23	1.342	0.89	2.013	0.12
120	0.75	0.29	1.5	0.81	2.25	1
130	0.821	0.23	1.643	0.78	2.464	1
140	0.883	0.25	1.766	0.53	2.649	1

more accurately the "θ_1-θ_2 converter," is designed to have an emerging beam with a maximum angle of 60°. Because of this wide angular spread, only 44% of the beam hits the detector. Thus, the previously quoted theoretical concentration of 56 is reduced to an effective value of about 24, in good agreement with the measured value of 23. This correction does not depend on the angular position of the detector in the array. The second source of loss is reflection from the two surfaces of the crystalline quartz window, which has a refractive index of $n = 2.1$. For an observer at infinity and in the $\phi = 0°$ plane, SP radiation would be completely polarized in the *x-z* plane. This is not strictly true for the present experimental conditions, but assuming that no significant error is introduced by making this approximation, it can be calculated by means of Fresnel's formulas that the transmitted power is about 55% at an incident angle of 50° (i.e. for $\theta = 40°$ and $\theta = 140°$). At normal incidence, this fraction increases to about 77%. The third correction reflects the fact that as the observation angle changes from 90° to 140° (or 40°), the effective grating length increases by $1/\sin\theta$, due to the increasing field of view of the detector. It is assumed that at these wavelengths the reflectivity of the cone material is perfect. It is has also been assumed that there is 100% transmission of the far-infrared radiation through the quartz window. Losses by absorption in air must be negligible due to the short path length and the absence of strong absorption lines in this wavelength region. The partial obstruction of the detectors at the two extreme angular positions has been taken into account in our calculations.

As indicated in the previous section, a small error was introduced by inaccuracies in the positioning of the blank and the gratings, relative to the beam axis. Specifically, it was found that, for the same nominal position of gratings and blank, the latter was actually closer to the beam axis by as much as 0.22 mm, thus increasing the x-ray background.

Based on a series of measurements with the blank, taken at varying distances from the axis, an appropriate correction factor was calculated and applied to the blank readings. The two remaining factors are the relative efficiencies of the detectors and their absolute calibration. The relative efficiencies of all detectors were checked by means of a Nd-YAG laser operating at 1064 nm and were found to be within $\pm 20\%$ of each other. An absolute calibration of 5.3 V/W at 130 μm was obtained by means of the FIR beam at FELIX. The question of the wavelength responsivity of pyroelectric detectors is more difficult to answer. There has been some experimental evidence from detectors that were similar but not identical to ours, that in the wavelength region 200–500 μm, the responsivity exhibits interferencelike fringes and may vary by as much as a factor of 5 [22]. Since the mechanism proposed by the authors of [22] (multiple reflections on the crystal surfaces) depends critically on material thickness, electrode conductivity, etc., it is impossible to extrapolate reliably to our detectors and our wavelength region. A purely empirical extrapolation of the data of Ref. [22] to the wavelength region 500–2500 μm suggests that the intensity variations in the interference fringes may have decreased to about $\pm 20\%$ of the average value. This uncertainty will appear as an increase in the systematic error.

The final consideration is the overall error in these measurements. In addition to the previously mentioned $\pm 20\%$ due to the detector wavelength responsivity, there could be systematic errors due to the filter transmission efficiency, the influence of the cone-detector separation and the reflection losses. All three are roughly of the order of $\pm 10\%$ each, giving an overall systematic error of about $\pm 30\%$. The statistical errors are likely to be dominated by the x-ray background, which will vary with small variations of beam position with time. A minimum figure of ± 5 mV was determined in the previous section. Its effect will be much more pronounced in the forward directions, where it determines the limit for this experiment. In the very backward directions and the 1.5 mm grating, an error of $(+0$–$10\%)$ has been estimated. The results of this analysis from all three gratings are combined in a single plot (Fig. 7) of measured SP power, all corrections included, against wavelength (order 1). The vertical error bars represent the total error. The uncertainty $d\theta$ in the observation angle is translated into a wavelength uncertainty by $\Delta\lambda = l\sin\theta d\theta$. Two points, both at $\theta = 90°$, but with different grating periods ($l = 1.0$ mm and $l = 1.5$ mm) have a horizontal error bar, to indicate this error. Different symbols have been used for the three gratings. With the exception of the 0.5 mm points, each of the other points represents the average of a number of runs, taken over a period of hours. A cut was placed at a signal level of 5 mV, which corresponds to about 4 mW at the detector. Points below that level (shaded area of Fig. 7) were removed from the analysis. There is no detectable SP signal
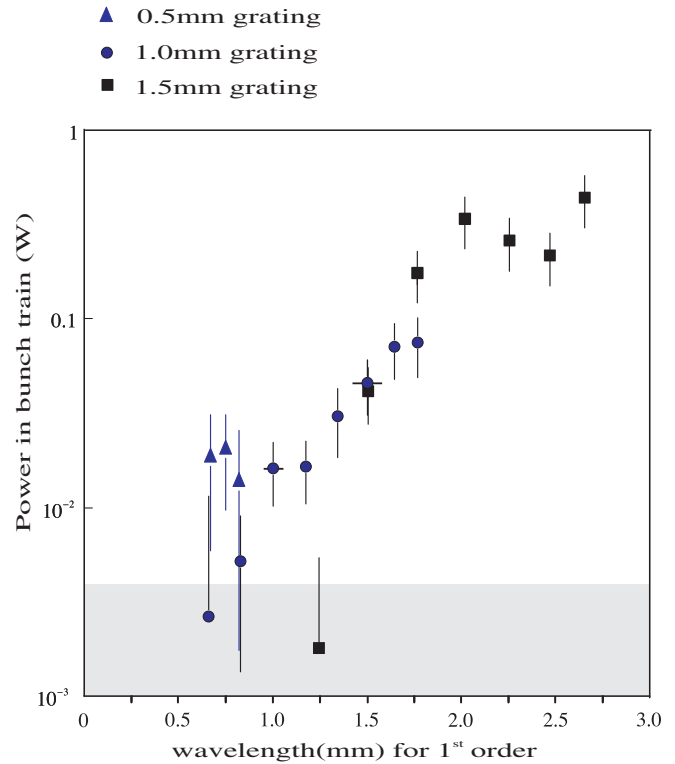

FIG. 7. (Color) Measured Smith-Purcell power versus 1st order wavelength from three different gratings. Beam energy was 45 MeV and bunch spacing 1 ns. Points in the shaded area have been excluded from the analysis. See text for details.

for wavelengths shorter than about 0.75 mm but above that, the signal increases steeply with increasing wavelength. Since long wavelengths are needed to bring the radiation into the coherent regime, the first observation is that the bunch length must be at the upper end of its expected range of 1–3 ps and, possibly, longer. This plot is the basis for the determination of the longitudinal profile of the bunch.

C. Bunch shape determination

Two alternative approaches can be used in order to determine the bunch profile. The first is to consider the data points as the Fourier transform of the bunch temporal profile and to do an inverse transform in order to derive that profile. Since there is no phase information available, this would yield the nearest symmetric bunch shape. The procedure used in this section is, essentially, the inverse of the above: the Fourier transforms of a number of profiles have been calculated and combined with the other terms in Eqs. (3a) and (3b), in order to derive the expected output for that particular profile. This is then compared to the measured points and the process repeated until the best fit is arrived at. This approach has the advantage that it can allow comparisons with "asymmetric" temporal profiles but it does assume some prior knowledge of the bunch length otherwise the fitting process would be excessively long. Nevertheless, the absence of phase information pre-

cludes the *unique* determination of an asymmetric profile. The analysis is carried out by means of two codes. The first uses the known beam and grating parameters and the assumed temporal profile, in order to calculate the differential energy (J/sr/cm) radiated as Smith-Purcell radiation. The physical basis for the calculation is the "surface current" treatment of the emission process [10–12]. The results from this code are then transferred to a second code that determines the solid angle $d\Omega$ (~ 1.4 msr), the effective grating length and the range of θ and ϕ angles accepted by the system ($\pm 3°$ and $\pm 4°$, respectively). It then averages the differential energy and arrives at a figure for the radiated energy. Finally, division of the energy by the bunch spacing yields the power expected to enter the detectors at a given wavelength.

A number of such wavelength distributions, arising from different temporal profiles, are shown in Figs. 8(a) and 8(b) in order to demonstrate the discrimination that can be expected. All temporal profiles have been assumed to be symmetric, relative to a reference particle at $t = 0$. Those in 8(a) are for bunch lengths of 5 ps while those in 8(b) for 6 ps; on the basis of the data of Fig. 7, these bunch lengths seem plausible. The plotted curves refer to 1st order emission and higher orders have been neglected. The calculations are based on the current experimental parameters and on the 1.5 mm grating. In all cases the radiated power rises steeply with wavelength. However, the spectral distributions of profiles with sharp "edges" (e.g. triangular) are nonmonotonic; this is due to their harmonic components. Clear separation between these profiles is possible, provided that the distribution can be measured over a reasonably wide range of wavelengths. Note, for example, that the power radiated into the detectors from a 5 ps Gaussian bunch would be about 150 mW at 1.5 mm, whereas a 6 ps Gaussian would radiate about 30 mW at the same wavelength. Measurements in the wavelength region where the radiation rises above the incoherent regime are particularly important. On the other hand, measurements in the long ($\lambda > 2.5$ mm) wavelength region are not very informative since the radiation approaches full coherence and the longitudinal profile of the bunch is irrelevant; the bunch begins to look like a point lump of charge.

Figures 9(a) and 9(b) show the same data points as Fig. 7, except for those in the shaded area which were removed from the analysis. The data have been fitted with a Gaussian and a slightly asymmetric triangular profile. In Fig. 9(a) the bunch length has been taken to be 5 ps, while in Fig. 9(b) it is 5.5 ps. Since the data points were derived from three different gratings, with different grating efficiency factors R^2 [see (2a) and (2b)], the curves are composites created by superposition of three separate curves, one for each grating. Clearly, an exponential shape can be excluded because the power levels are too low [see Figs. 8(a) and 8(b)]. The possibility of a simple Gaussian shape can also be excluded since, if that were the case, the
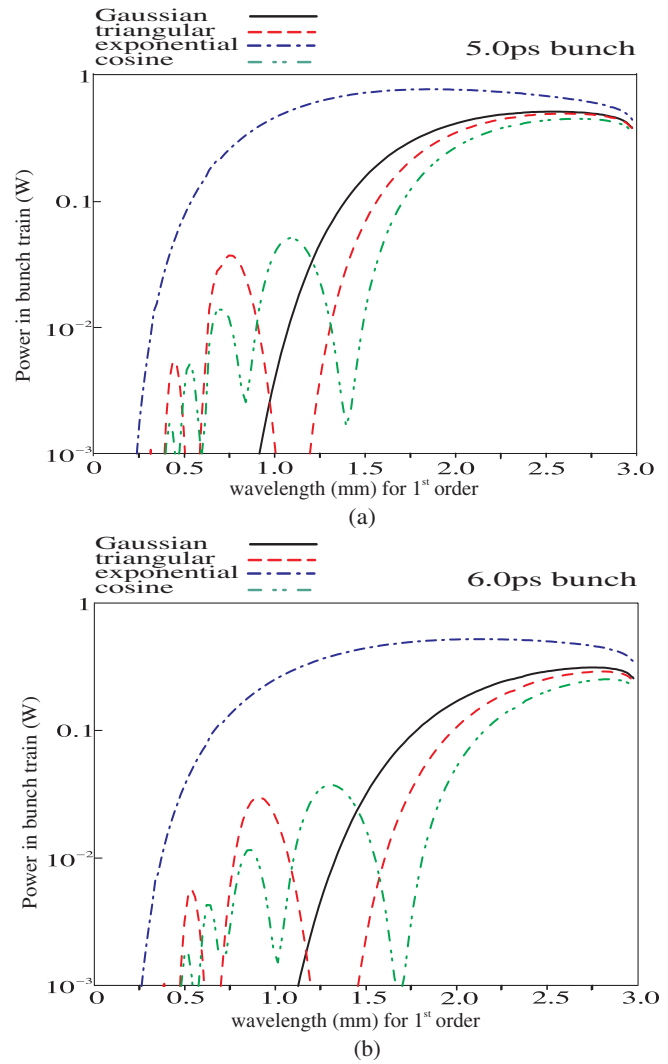

FIG. 8. (Color) Plots of the expected wavelength distribution of Smith-Purcell radiation for a number of bunch profiles. The bunch length (90% of particles) has been taken to be equal to 5 ps in (a) and 6 ps in (b).

power would have dropped below the detectable level at a wavelength of about 1 mm. Within the accuracy of the experiment the measured wavelength distribution is consistent with an approximately triangular profile, with 90% of the bunch particles contained inside 5.5 ps. This bunch profile, together with the Gaussian, is shown in the insert of Fig. 9(b).

As stated earlier, the work presented here is for 1st order emission because it has not been possible to explore higher orders. There is always the possibility that some of the power measured at a given observation port could be due to, say, the 2nd order that is "leaking" through the filter. This is unlikely to introduce a significant error in the analysis because the power in $m = 2$ is probably lower and, in any case, the WAP filters do provide some suppression for wavelengths shorter than the central one. The transmission efficiency of the filter of Fig. 4(a), for ex-
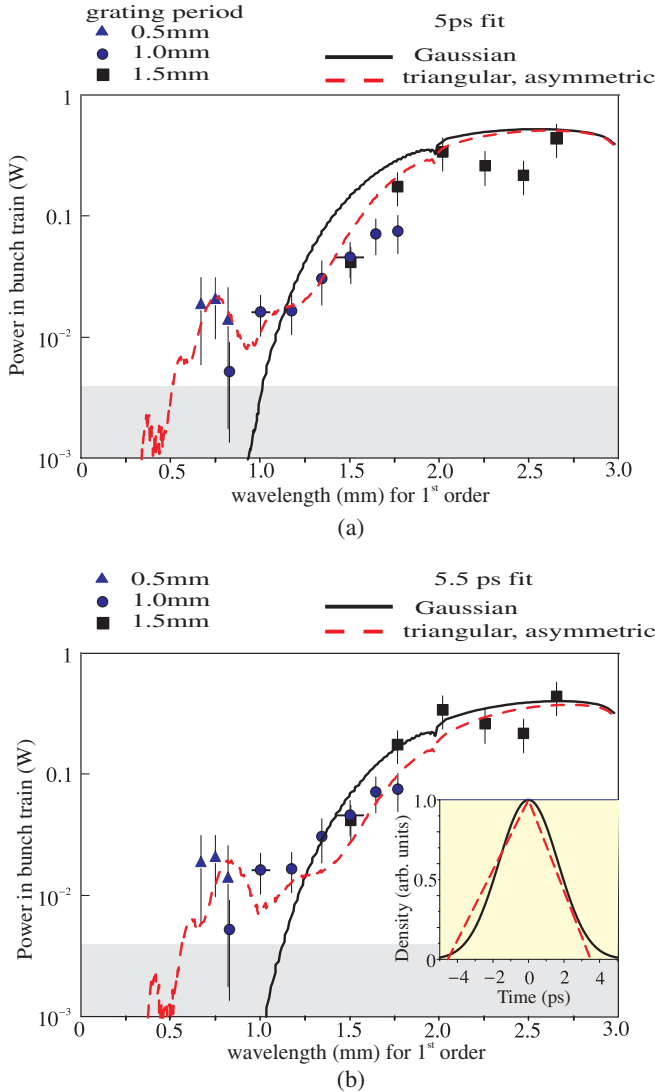
FIG. 9. (Color) The data points of Fig. 7 fitted with a Gaussian and an asymmetric triangular profile, with 90% of the particles contained inside (a) 5 ps and (b) 5.5 ps. The inset in (b) shows these two bunch profiles.

ample, drops to about 15%–20% of its peak value when the wavelength is halved. This is typical for all these filters and, therefore, the error introduced by ignoring the contribution of $m = 2$ is well within the systematic error. Nevertheless, the availability of suitable WAP filters and a reduction in the systematic errors could make possible the measurement of the power radiated at $m > 1$. Under certain circumstances, e.g., bunch length much shorter than the grating period, this could be significant and it could extend the accessible range of wavelengths.

IV. SUMMARY AND CONCLUSIONS

We have extended our previous work on coherent Smith-Purcell radiation by a factor of 10 in energy and a factor of 3–5 towards shorter bunch lengths. An array of 11 pyro-

electric detectors provided simultaneous detection of the SP radiation in the angular range 40°–140° relative to the electron beam direction. The absence of any external spectrometer for the identification of SP radiation necessitates particular attention to the measurement and subtraction of the non-SP background radiation. This has been achieved through the use of high quality FIR filters, nonimaging light concentrators, and a carousel arrangement, carrying three gratings of different periodicities plus a plain piece of metal (blank). Use of high quality band pass filters ("waveguide array plates") provides excellent rejection of the unwanted wavelengths, especially in the long wavelength region. This type of filter is more difficult and expensive to manufacture but its performance is far superior to that of conventional fine wire mesh filters. It also offers the possibility of investigating SP radiation for orders $m > 1$. The second critical component in the optical system was the specially designed nonimaging light concentrator ("Winston cone"). Use of the Winston cone not only improves the light collection efficiency but it also provides additional discrimination against the background, especially at long wavelengths. Finally, the carousel allowed for rapid grating changes and for subtraction of the contribution of the blank, which had dimensions identical to those of the gratings but without any periodicity. To the best of our knowledge, this is the first measurement of the average power in the bunch train done entirely by means of room-temperature detectors and carefully designed electronics.

One of the main objectives of future experimental work should be the reduction of the error bars. As far as statistical errors are concerned, the accuracy of the present system is limited to ± 5 mV of detector output. This is determined primarily by the x-ray background from the beam halo and, possibly, from the nearby beam dump. In view of the fact that the detector itself is about 3 orders of magnitude less sensitive to x rays than its electronics, it is possible to achieve significant reduction in this figure by decoupling the electronics from the detector and moving it further away from the beam line. Another cause of statistical uncertainty is a possible small drift in beam position over time. A faster and more accurate system for changing between gratings and blank would address this problem. Work is already in progress regarding both these issues. Reduction of the systematic errors is a more challenging problem, the main difficulty being the accurate calibration of the detectors against wavelength. It is possible to use SP radiation to cross-calibrate the detectors at a number of wavelengths by rotation of the various detectors along the 11 observation ports. Absolute measurements of power in the far infrared are, however, difficult. The requirement here is for an absolute calibration method of at least one detector over a series of wavelengths in the wavelength region of the experiment. SP radiation could provide a partial answer to this problem by using one detector over

a range of observation angles where the radiation is *fully coherent*. The assumption here is that the power level is more or less constant but the wavelength changes, although over a limited range.

We conclude that, within the accuracy of the system, the length of the FELIX bunch, at the position where it was measured, is about 5.5 ps; "bunch length" is defined as the time interval containing 90% of the bunch particles. If the bunch were Gaussian in temporal profile, this would correspond to a standard deviation of 1.6 ps. The bunch shape, however, is not Gaussian but *may* approximate that of a triangular shape, slightly asymmetric relative to the reference particle. We note again that this conclusion has been reached by comparison of the measured distribution with various "templates" corresponding to a number of assumed, simple bunch profiles and cannot be considered as unique. We are pursuing alternative methods for extracting the profile from the wavelength distribution of the radiation, through the development of a computer code that would allow for far faster and more detailed comparisons between data and possible profiles. Furthermore, a data acquisition system would simplify greatly data collection and analysis, including the application of the various correction factors. These improvements, together with the inherently simple, compact, and robust experimental arrangement and the nonintercepting character of SP radiation, make this process a very promising candidate for the determination of the bunch profile for any charged particle beam, over a very wide range of energies. Further experimental work at higher beam energies, shorter bunch lengths, and higher orders is highly desirable.

Finally, and in view of recent discussions on the various theoretical treatments of Smith-Purcell radiation [10,13,23,24], we note that the measured power levels are entirely in line with the predictions of the "surface current" model and we see no reason at present for any changes to the theoretical treatment. A detailed comparison of the data with the predictions of alternative theories is under way [25].

[1] S. J. Smith and E. M. Purcell, Phys. Rev. **92**, 1069 (1953).

[2] G. Doucas, M. F. Kimmitt, A. Doria, G. P. Gallerano, E. Giovenale, G. Messina, H. L. Andrews, and J. H. Brownell, Phys. Rev. ST Accel. Beams **5**, 072802 (2002).

[3] G. Doucas, M. F. Kimmitt, A. Doria, G. P. Gallerano, E. Giovenale, G. Messina, H. L. Andrews, and J. H. Brownell, *Proceedings of the 8th European Particle Accelerator Conference, Paris, 2002* (CERN, Geneva, 2002), p. 1870.

[4] S. E. Korbly, A. S. Kesar, R. J. Temkin, and J. H. Brownell, Phys. Rev. ST Accel. Beams **9**, 022802 (2006).

[5] P. Chen and K. Yokoya, Phys. Rev. D **38**, 987 (1988).

[6] G. Toraldo di Francia, Il Nuovo Cimento **16**, 61 (1960).

[7] P. M. van den Berg, J. Opt. Soc. Am. **63**, 689 (1973).

[8] P. M. van den Berg, J. Opt. Soc. Am. **63**, 1588 (1973).

[9] O. Haeberlé, P. Rullhusen, J. M. Salomé, and N. Maene, Phys. Rev. E **49**, 3340 (1994).

[10] J. H. Brownell, J. E. Walsh, and G. Doucas, Phys. Rev. E **57**, 1075 (1998).

[11] S. R. Trotz, J. H. Brownell, J. E. Walsh, and G. Doucas, Phys. Rev. E **61**, 7057 (2000).

[12] J. H. Brownell and G. Doucas, Phys. Rev. ST Accel. Beams **8**, 091301 (2005).

[13] G. Kube, H. Backe, H. Euteneuer, A. Grendel, F. Hagenbuck, H. Hartmann, K. H. Kaiser, W. Lauth, H. Schöpe, G. Wagner, Th. Walcher, and M. Kretzschmar, Phys. Rev. E **65**, 056501 (2002).

[14] C. Winnewisser, F. Lewen, J. Weinzierl, and H. Helm, Appl. Opt. **38**, 3961 (1999).

[15] F. Keilmann, Int. J. Infrared Millim. Waves **2**, 259 (1981).

[16] E. Castro-Camus, J. Lloyd-Hughes, M. B. Johnston, M. D. Fraser, H. Tan, and C. Jagadish, Appl. Phys. Lett. **86**, 254102 (2005).

[17] M. L. Oldfield, B. N. Ellison, B. J. Maddison, C. M. Mann, B. P. Moyna, and D. N. Matheson, Int. J. Infrared Millim. Waves **18**, 1547 (1997).

[18] W. T. Welford and R. Winston, *The Optics of Non-imaging Concentrators: Light and Solar Energy* (Academic Press, New York, 1978), ISBN: 0127453504.

[19] R. H. Hildebrand and R. Winston, Appl. Opt. **21**, 1844 (1982).

[20] G. Doucas, S. Gil, N. A. Jelley, L. McGarry, M. E. Moorhead, N. W. Tanner and C. E. Waltham, Nucl. Instrum. Methods Phys. Res., Sect. A **370**, 579 (1996).

[21] U. Happek, A. J. Sievers, and E. B. Blum, Phys. Rev. Lett. **67**, 2962 (1991).

[22] W. Zhu, J. R. Izatt, and B. K. Deka, Appl. Opt. **28**, 3647 (1989).

[23] A. S. Kesar, M. Hess, S. E. Korbly, and R. J. Temkin, Phys. Rev. E **71**, 016501 (2005).

[24] A. S. Kesar, Phys. Rev. ST Accel. Beams **8**, 072801 (2005).

[25] A. S. Kesar and J. H. Brownell (private communication).